Available online at www.garmian.edu.krd

Passer Journal of Basic and Applied Sciences

Passer 7 (Issue 2) (2025) 765-782

Original Article

A New Extending Inverse Weibull Distribution to Handle Neutrosophic Logic: Mathematical Properties, Parameter Estimation, and Simulation with Application

Kamal N. Abdullah * [1], Mundher A. Khaleel [1]

[1] *Mathematics Departments, College of Computer Science and Mathematics, Tikrit University, Iraq.*

Received 13 April 2025; revised 02 August 2025;
accepted 09 February 2025; available online 03 April 2025

DOI: 10.24271/psr.2025.516585.2073

ABSTRACT

The study aims to introduce a new extension of the inverse Weibull distribution, developed within the modified Weibull (MWG) family, to address uncertainty in neutrosophic logic. This new model is called the Neutrosophic Modified Weibull Inverse Weibull (NMWIW) distribution. The mathematical properties of the proposed distribution, including its density, cumulative distribution, and survival functions, were analyzed, with parameter estimation using three methods (MLE, LSE, and WLSE). Monte Carlo simulation demonstrated the superiority of the MLE method in terms of estimation accuracy to the MSE, RMSE, and BIAs criteria. The model was applied to two datasets: the daily COVID-19 death rate in the Netherlands (March 31 – April 30, 2020) and the estimated under-five child mortality periods. The result demonstrated the superiority of the NMWIW compared to six other distributions (e.g., NBIW, NKIW) using information criteria (AIC, BIC) and statistical measures (K-S, p-value), proving its effectiveness in modeling real-world data under uncertain conditions. The graphs also confirmed the model's fit to the experimental data, making it a powerful tool for risk analysis and decision-making in the presence of ambiguous data.

Keywords: Modified Weibull family, Inverse Weibull, neutrosophic logic, crude mortality rate, and COVID-19.

1 Introduction

Continuous distribution is essential in statistical data analysis, particularly in reliability, forecasting, and risk assessment. The Weibull distribution, recognized for its versatility in modeling diverse data patterns, has been extensively modified to broaden its applicability. Additionally, the Inverse Weibull distribution provides further benefits in analyzing data characterized by high variability or non-constant failure rates. However, despite the adaptability of these distributions, they remain constrained in their capacity to analyze various data types. In recent years, the field of statistical has witnessed significant growth in the development of new distributions, introducing families of continuous distributions designed to enhance flexibility and adaptability to complex data.

This methodology addresses data that exhibit atypical behavior, encompass ambiguity, missing values, or volatility. Examples of these families include: Kumaraswamy transmuted-G family (Kw-TG) [1], odd exponentiated half-logistic-G family (OEHL-G) [2], Extended odd Frechet-G family (EOF-G) [3], generalized odd inverted exponential-G family (GOIE-G) [4], modified alpha power Weibull-X family (MAPW-X) [5], Odd Lomax-G (LOG) [6], Odd Generalized Exponentiated Exponential-G Family (NOGEE−G) [7], generalized logarithmic–X family (NGLog-X) [8], type I half Logistic exponentiated-G (TIHL) [9], and hybrid odd exponential-Φ (HOE-Φ) [10].

Neutrosophic logic has garnered significant interest in addressing uncertainty and ambiguity in data. It comprises three elements: Truth, Falsity, and indeterminacy, which can coexist inside the same system. This logic was initially introduced by Smarandache in 1999 [11]. It diverges from conventional approaches that depend on three distinct components by broadening the range of random variables, parameters, or data to address them in the form of intervals, hence improving accuracy and flexibility in data analysis. A restricted number of statistical distributions have been combined with neutrosophic logic.

Examples that appear in references [12], [13], [14], [15], [16], and [17].

The modified Wiebull family was created to offer versatile expansions of neutrosophic distribution. The suggested novel distribution is fundamentally based on one of the first families of statistical distributions designed to manage ambiguous data. This

* Corresponding author
E-mail address kn230022pcm@st.tu.edu.iq (Other).
Peer-reviewed under the responsibility of the University of Garmian.

family possesses a neutrosophic cumulative density function (NCDF) and neutrosophic probability density function (NPDF), delineated by the subsequent equation, respectively:

$$G_{NMW}(x_N) = 1 - e^{-r_N\left(\frac{(F(x_N))^2}{1-F(x_N)}\right)^{u_N}} \quad (1)$$

$$g_{NMW}(x_N) = r_N u_N e^{-r_N\left(\frac{(F(x_N))^2}{1-F(x_N)}\right)^{u_N}} \left(\frac{(F(x_N))^2}{1-F(x_N)}\right)^{u_N-1} \frac{F(x_N)f(x_N)(2-F(x_N))}{(1-F(x_N))^2} \quad (2)$$

In the context of the neutrosophic Modified Wiebull (NMWIW) family, r_N and u_N represent the neutrosophic shape parameters, constrained by $r_N \in [r_L, r_U]$ and $u_N \in [u_L, u_U]$, where r_L and u_L denote the lower bounds and r_U, u_U denote the upper bounds of these parameter. Additionally, X_N is defined as $X_N = d + tI$, $tI \in [X_L, X_U]$ where X_L, X_U signify the lower and upper limited of the neutrosophic random variable. Furthermore, $F(x_N), f(x_N)$ correspond to the neutrosophic cumulative density function (NCDF) and neutrosophic probability density function (NPDF) for any baseline neutrosophic distribution.

The gap in the literature is the lack of effect statistical models capable of handling fuzzy and uncertain data, especially in the context of analyzing COVID-19 mortality data and interval estimates of infant death rates for the age less than five years, also most the proposed neutrosophic distributions are basic distribution that were developed to deal with neutrosophic logic, i.e. they were not combined to add more neutrosophic parameters to give greater flexibility in dealing with uncertain data.

This study aims to bridge this gap by developing an inverse Weibull distribution within the NMWG family, incorporating neutrosophic concepts and introducing various properties of this distribution to show the nature of the proposed model, with figures and tables to illustrate the findings.

The importance of this study lies in presenting a new statistical model with high flexibility and efficiency in parameter estimation, while improving the accuracy of predictions and risk analysis, which contributes to improved decision-making in the face of uncertain data.

2 Neutrosophic Modified Weibull Inverse Weibull (NMWIW) distribution

Take x be any random variable, then the CDF function for Inverse Weibull (IW) has a form $F(x; a, b) = e^{-ax^{-b}}$, $a, b, x > 0$, and pdf with form $f(x; a, b) = abx^{-(b+1)}e^{-ax^{-b}}$ [18].

Definition: Let the $X_N = d + tI$, $tI \in [X_L, X_U]$, where X_L, X_U are lower and upper values of the Neutrosophic Inverse Weibull (NIW) distribution random variable having determined part d and indeterminate part tI, $tI \in [I_L, I_U]$. Note that the NIW reduces to classical Inverse Weibull when $X_L = X_U$. The neutrosophic cumulative density (NCDF), and neutrosophic probability density (Npdf) of NIW has a Neutrosophic shape parameters $a_N \in [a_L, a_U]$, $b_N \in [b_L, b_U]$, has the form:

$$F(x_N, a_N, b_N) = e^{-a_N x_N^{-b_N}} \quad (3)$$

$$f(x_N, a_N, b_N) = a_N b_N x_N^{-(b_N+1)} e^{-a_N x_N^{-b_N}} \quad (4)$$

The NCDF function of NMWIW with four neutrosophic parameters and a neutrosophic random variable is obtained by combining equation 1 with equation 3 to obtain an equation in the form:

$$G(x_N) = 1 - e^{-r_N\left(\frac{\left(e^{-a_N x_N^{-b_N}}\right)^2}{1-e^{-a_N x_N^{-b_N}}}\right)^{u_N}}, \qquad x_N, r_N, u_N, a_N, b_N > 0 \quad (5)$$

To find out how this function fits NMWIW distribution, the NCDF function is plotted using R programing with different values for parameters intervals.

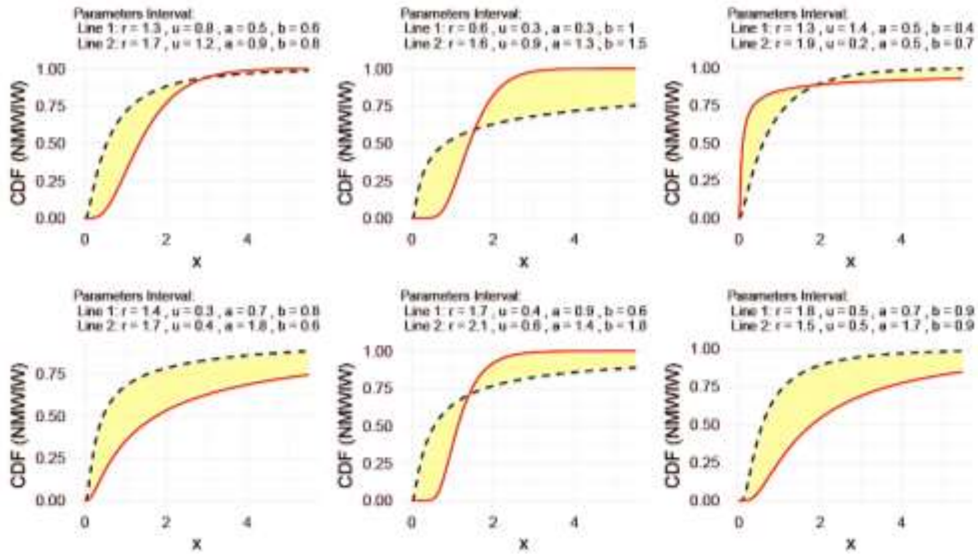

Figure 1: Plot NCDF function for NMWIW distribution.

Each graph shows two curves: a red line representing the lower bound of the function and a dashed black line representing the upper bound of the function. The yellow shaded area between the two lines represents the neutrosophic uncertainty region. The figures show a wide range of cumulative function curves, highlighting the distribution's capability to adapt to diverse data patterns. The curves range from steep to gradual, demonstrating the distribution's ability to capture data behavior from narrow to long-tailed distributions.

Now, to find the Npdf function for NMWIW distribution, we will derivative equation (5), to get a final form:

$$g(x_N) = r_N u_N a_N b_N x_N^{-(b_N+1)} e^{-a_N x_N^{-b_N}} \left(2 - e^{-a_N x_N^{-b_N}}\right) \frac{\left(e^{-a_N x_N^{-b_N}}\right)^{2u_N-1}}{\left(1-e^{-a_N x_N^{-b_N}}\right)^{u_N+1}} \times e^{-r_N\left(\frac{\left(e^{-a_N x_N^{-b_N}}\right)^2}{1-e^{-a_N x_N^{-b_N}}}\right)^{u_N}} \tag{6}$$

To evaluate how this function fits the NMWIW distribution, the Npdf function is plotted using R programming with different parameter intervals.

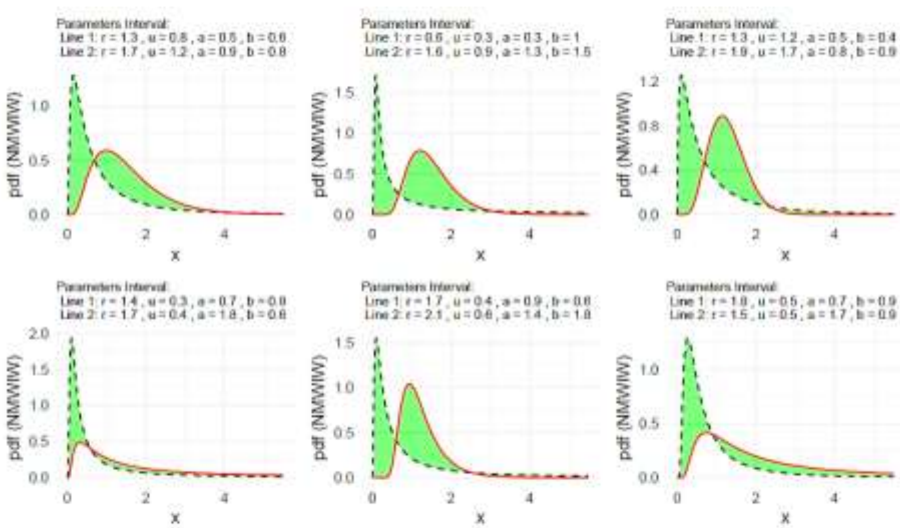

Figure 2: Plot Npdf function for NMWIW distribution.

As shown in Figure 2, some graphs exhibit a sharp peak that quickly fades, indicating that data are concentrated around small values and have a low probability of large values. This pattern is observed when the b_N parameter takes low values, which controls the shape of the tail. The flexibility of the distribution parameters enables the NMWIW to effectively represent a wide range of complex data. Therefore, the distribution is well-suited for datasets characterized by uncertainty or ambiguity, such as those found in physical, financial, or environmental systems.

The neutrosophic Survival function can be getting in form [19]:

$$S(x_N) = 1 - G(x_N)$$

$$S(x_N) = e^{-r_N\left(\frac{\left(e^{-a_N x_N^{-b_N}}\right)^2}{1-e^{-a_N x_N^{-b_N}}}\right)^{u_N}} \tag{6}$$

In the same way that the NCDF and Npdf function draws for a distribution, the neutrosophic Survival function for NMWIW distribution is drawn. Figure 3 represents a set of shapes for the neutrosophic Survival function for NMWIW.

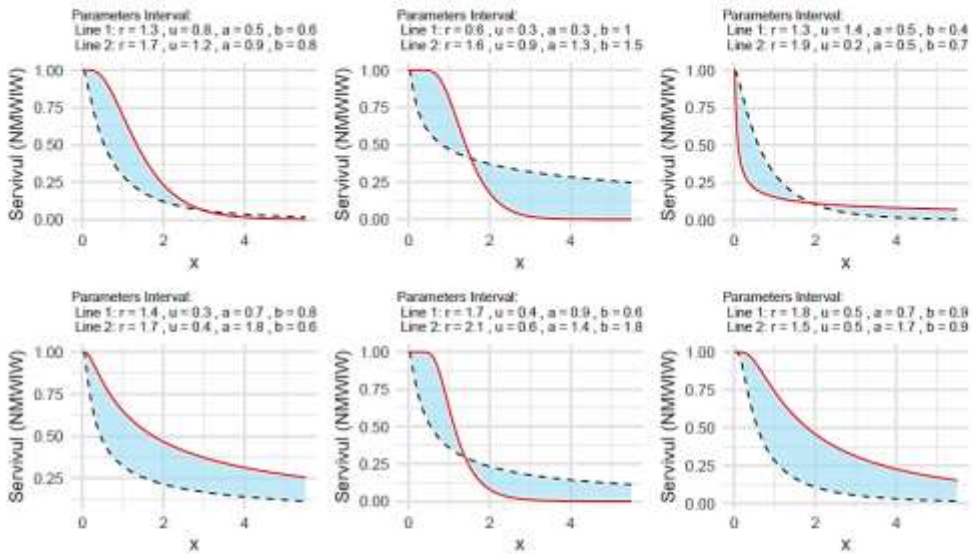

Figure 3: Plot neutrosophic Survival function for NMWIW distribution.

Figure 3 shows that, in all graphs, the survival function decreases as the values of the random variable increase, reflecting the probability of an event lasting longer before failure or termination occurs. Some figures show a slight upward trend or a delayed decline, indicating an initially stable system before deterioration occurs. In other cases, there is a sharp initial decline, followed by gradual stabilization, which is common in system with sudden failures or system sensitive to external factors. The variation in figures reflects the flexibility to handle data with different patterns of failure or success.

The neutrosophic hazard function can be obtained in form [19]:

$$h(x_N) = \frac{g(x_N)}{S(x_N)}$$

$$h(x_N) = r_N u_N a_N b_N x_N^{-(b_N+1)} e^{-a_N x_N^{-b_N}} \left(2 - e^{-a_N x_N^{-b_N}}\right) \frac{\left(e^{-a_N x_N^{-b_N}}\right)^{2u_N - 1}}{\left(1 - e^{-a_N x_N^{-b_N}}\right)^{u_N+1}} \tag{7}$$

In most cases, the previous functions in their current form are difficult to prove for statistical distribution properties. Therefore, these functions are expanded using binomial and exponential series to derive simpler equations. Hence the NCDF function shown in equation 5 is derived in an expanded form:

$$G(x_N) = 1 - M\left(e^{-(2i_N u_N + j_N) a_N x_N^{-b_N}}\right) \tag{9}$$

where $M = \sum_{i_N = j_N = 0}^{\infty} \frac{(-1)^{i_N} \Gamma(i_N u_N + j_N) r_N^{i_N}}{i_N! j_N! \Gamma(i_N u_N)}$.

And the CDF^{δ_N}, which has a form:

$$G^{\delta_N}(x_N) = \left(1 - e^{-r_N\left(\frac{\left(e^{-a_N x_N^{-b_N}}\right)^2}{1-e^{-a_N x_N^{-b_N}}}\right)^{u_N}}\right)^{\delta_N} \tag{8}$$

Which has the expanded form:

$$G^{\delta_N}(x_N) = \Upsilon e^{-(2t_N u_N + s_N) a_N x_N^{-b_N}} \tag{9}$$

where $\Upsilon = \sum_{k_N=t_N=s_N=0}^{\infty} \frac{(-1)^{t_N+k_N}\Gamma(t_N u_N+s_N)}{t_N! s_N! \Gamma(t_N u_N)} \binom{\delta_N}{k_N} r_N^{t_N} k_N^{t_N}$.

The Npdf function shown in equation 6 is obtained in an expanded form:

$$g(x_N) = 2\varphi x_N^{-(b_N+1)} e^{-(2u_N(n_N+1)+z_N+1)a_N x_N^{-b_N}} - \varphi x_N^{-(b_N+1)} e^{-(2u_N(n_N+1)+z_N+2)a_N x_N^{-b_N}} \quad (12)$$

3 Some Properties for NMWIW Distribution

3. 1 Neutrosophic Quantile function for NMWIW distribution

Theorem: Let $G(x_N)$ be an NCDF of NMWIW distribution, where $G(x_N): \mathbb{R} \to [0,1]$ is monotonically increasing and non-decreasing. Then the Neutrosophic Quantile function $Q(p_N)$ for NMWIW distribution has the form:

$$Q(p_N) = \left(-\frac{a_N}{\log(B)}\right)^{\frac{1}{b_N}} \quad (10)$$

where $B = \frac{-\left(\frac{-\log(1-p_N)}{r_N}\right)^{\frac{1}{u_N}} \mp \sqrt{\left(\frac{-\log(1-p_N)}{r_N}\right)^{\frac{2}{u_N}} - 4\left(\frac{-\log(1-p_N)}{r_N}\right)^{\frac{1}{u_N}}}}{2}$

Proof: assume that $p_N = G(x_N)$ [20].

Then $p_N = 1 - e^{-r_N\left(\frac{\left(e^{-a_N x_N^{-b_N}}\right)^2}{1-e^{-a_N x_N^{-b_N}}}\right)^{u_N}} \Rightarrow 1 - p_N = e^{-r_N\left(\frac{\left(e^{-a_N x_N^{-b_N}}\right)^2}{1-e^{-a_N x_N^{-b_N}}}\right)^{u_N}}$

Take the log for both sides to get: $\frac{-\log(1-p_N)}{r_N} = \left(\frac{\left(e^{-a_N x_N^{-b_N}}\right)^2}{1-e^{-a_N x_N^{-b_N}}}\right)^{u_N}$

Take raise both sides to strength $(\frac{1}{u_N})$ to get:

$$\left(\frac{-\log(1-p_N)}{r_N}\right)^{\frac{1}{u_N}} = \frac{\left(e^{-a_N x_N^{-b_N}}\right)^2}{1-e^{-a_N x_N^{-b_N}}}$$

But $z = e^{-a_N x_N^{-b_N}}$, and

$\left(\frac{-\log(1-p_N)}{r_N}\right)^{\frac{1}{u_N}} = a \Rightarrow a = \frac{z^2}{1-z} \Rightarrow z^2 + az - a = 0$, Solve the quadratic equation for $z \Rightarrow z = \frac{-a \mp \sqrt{a^2-4a}}{2}$

$$\Rightarrow e^{-a_N x_N^{-b_N}} = \frac{-\left(\frac{-\log(1-p_N)}{r_N}\right)^{\frac{1}{u_N}} \mp \sqrt{\left(\frac{-\log(1-p_N)}{r_N}\right)^{\frac{2}{u_N}} - 4\left(\frac{-\log(1-p_N)}{r_N}\right)^{\frac{1}{u_N}}}}{2}$$

, put $\frac{-\left(\frac{-\log(1-p_N)}{r_N}\right)^{\frac{1}{u_N}} \mp \sqrt{\left(\frac{-\log(1-p_N)}{r_N}\right)^{\frac{2}{u_N}} - 4\left(\frac{-\log(1-p_N)}{r_N}\right)^{\frac{1}{u_N}}}}{2} = B$

$\Rightarrow -a_N x_N^{-b_N} = \log(B) \quad \Rightarrow x_N^{-b_N} = -\frac{\log(B)}{a_N} \Rightarrow -\frac{a_N}{\log(B)} = x_N^{b_N} \Rightarrow x_N = \left(-\frac{a_N}{\log(B)}\right)^{\frac{1}{b_N}}$

Finally, we get a form in equation 13 ∎.

The table below presents the values of the quintile function for the NMWIW distribution across different parameter intervals. The table shows the quintile values at different data ratios (0.1,0.2, …,0.9), which reflect the behavior of the data distribution under neutrosophic uncertainty. It helps in evaluating the data distribution and analyzing the variance between the minimum and maximum limits of the quintile values. It is used to identify extreme and marginal values, which contribute to risk analysis and forecasting future trends

Table 1: Quintile function of NHWIW distribution.

q_N	(r_N, u_N, a_N, b_N)				
	[0.8, 1.8],[0.9, 1.9] [0.4, 1.4],[0.7, 1.7]	[0.6, 1.6],[0.4, 1.4] [0.4, 1.4],[0.5, 1.5]	[0.5,1.5],[0.6.1,6] [0.5,1.5],[0.6,1.6]	[0.7,1.7],[0.5,1.5] [0.8,1.8],[0.7,1.7]	[0.7,1.7],[0.9,1.9] [0.7,1.7],[1,2]
0.1	[0.1882227,1.232230]	[0.03213967,1.133764]	[0.1727616,1.252484]	[0.2762149,1.319435]	[0.5710653,1.323785]
0.2	[0.2893752,1.356045]	[0.08389222,1.296360]	[0.3587393,1.407891]	[0.4986949,1.476257]	[0.7803135,1.436907]
0.3	[0.3976569,1.447024]	[0.19396431,1.423219]	[0.6451458,1.525895]	[0.8109997,1.595565]	[0.9832318,1.519116]
0.4	[0.5229873,1.525172]	[0.44530964,1.537307]	[1.1031428,1.629822]	[1.2820708,1.700826]	[1.2000698,1.589136]
0.5	[0.6755763,1.598192]	[1.06586410,1.648226]	[1.8613731,1.729046]	[2.0340806,1.801423]	[1.4455789,1.654082]
0.6	[0.8711293,1.670909]	[2.75264035,1.762826]	[3.1780501,1.829760]	[3.3150959,1.903768]	[1.7387029,1.718349]
0.7	[1.1391029,1.748140]	[7.97479666,1.889151]	[5.6436492,1.938841]	[5.7020015,2.014827]	[2.1119836,1.786158]
0.8	[1.5480518,1.837556]	[27.90018909,2.041247]	[10.9227020,2.06774]	[10.851891,2.146301]	[2.6367411,1.864113]
0.9	[2.3304461,1.959516]	[147.04781407,2.25871]	[26.1449980, .24789]	[26.017932,2.330562]	[3.5412133,1.969568]

From the table above, it is clear that quantitative values increase with increasing percentage q_N, indicating a wider spread in the data. There is also a clear discrepancy between the minimum and maximum values, reflecting the degree of uncertainty in the distribution parameter. For small values such as $q_N = 0.1$, the gap between the minimum and maximum values is relatively small, while for larger values, such as $q_N = 0.9$, it increases significantly. High percentage values indicate outliers, which can be useful in risk analysis or predicting rare events. The table demonstrates the flexibility of the NMWIW distribution in handling uncertain data, making it well-suited for analyzing real-world datasets characterized by ambiguity and uncertainty.

3. 2 Neutrosophic moment function for NMWIW distribution

Theorem: Let X_N be a neutrosophic random variable where $g(x_N)$ denotes the Npdf characterized by a neutrosophic Moment, then the neutrosophic Moment of the NMWIW distribution of order n has the form:

$$\mu_n = \frac{\varphi\Gamma\left(\frac{n-b_N}{b_N}\right)}{b_N a_N^{\frac{n-b_N}{b_N}}}\left[\frac{2}{(2u_N(n_N+1)+z_N+1)^{\frac{n-b_N}{b_N}}} - \frac{1}{(2u_N(n_N+1)+z_N+2)^{\frac{n-b_N}{b_N}}}\right] \tag{14}$$

Proof: let X_N be a neutrosophic random variable with $g(x_N)$ is Npdf, then the moment function has a form [21, 14, 12]:

$$\mu_n = E(x_N^n) = \int_{-\infty}^{\infty} x_N^n g(x_N)dx_N$$

Substituting equation (12) into the above equation yields a new form.

$$\mu_n = \int_{-\infty}^{\infty} x_N^n\left(2\varphi x_N^{-(b_N+1)}\left(e^{-a_N x_N^{-b_N}}\right)^{2u_N(n_N+1)+z_N+1} - \varphi x_N^{-(b_N+1)}\left(e^{-a_N x_N^{-b_N}}\right)^{2u_N(n_N+1)+z_N+2}\right)dx_N$$

$$\mu_n = \int_{-\infty}^{\infty} 2\varphi x_N^{n-(b_N+1)}\left(e^{-a_N x_N^{-b_N}}\right)^{2u_N(n_N+1)+z_N+1} - \varphi x_N^{n-(b_N+1)}\left(e^{-a_N x_N^{-b_N}}\right)^{2u_N(n_N+1)+z_N+2} dx_N$$

$$\mu_n = 2\varphi I_1 dx_N - \varphi I_2 dx_N$$

where $I_1 = \int_0^\infty x_N^{n-(b_N+1)}\left(e^{-a_N x_N^{-b_N}}\right)^{2u_N(n_N+1)+z_N+1} dx_N$

and $I_2 = \int_0^\infty x_N^{n-(b_N+1)}\left(e^{-a_N x_N^{-b_N}}\right)^{2u_N(n_N+1)+z_N+2} dx_N$

For I_1, let $y = (2u_N(n_N+1)+z_N+1)a_N x_N^{-b_N}$

$$x_N = \frac{y^{\frac{1}{b_N}}}{a_N^{\frac{1}{b_N}}(2u_N(n_N+1)+z_N+1)^{\frac{1}{b_N}}} \Longrightarrow dx_N = \frac{\frac{1}{b_N}y^{\frac{1}{b_N}-1}}{a_N^{\frac{1}{b_N}}(2u_N(n_N+1)+z_N+1)^{\frac{1}{b_N}}}dy$$

Then $I_1 = \int_0^\infty \left(\frac{y^{\frac{1}{b_N}}}{a_N^{\frac{1}{b_N}}(2u_N(n_N+1)+z_N+1)^{\frac{1}{b_N}}}\right)^{n-(b_N+1)} e^{-y}\frac{\frac{1}{b_N}y^{\frac{1}{b_N}-1}}{a_N^{\frac{1}{b_N}}(2u_N(n_N+1)+z_N+1)^{\frac{1}{b_N}}}dy$

Simplify I_1 to achieve the following final form:

$$I_1 = \frac{1}{b_N a_N^{\frac{n-b_N}{b_N}}(2u_N(n_N+1)+z_N+1)^{\frac{n-b_N}{b_N}}}\int_0^\infty y^{\frac{n-b_N}{b_N}-1}e^{-y}dy$$

$$I_1 = \frac{\Gamma\left(\frac{n-b_N}{b_N}\right)}{b_N a_N^{\frac{n-b_N}{b_N}}(2u_N(n_N+1)+z_N+1)^{\frac{n-b_N}{b_N}}}$$

In the same way for I_2 to get a final form:

$$I_2 = \frac{\Gamma\left(\frac{n-b_N}{b_N}\right)}{b_N a_N^{\frac{n-b_N}{b_N}}(2u_N(n_N+1)+z_N+2)^{\frac{n-b_N}{b_N}}}$$

Finally, we get a form in equation 14 ■.

From equation 14, the initial four moments are determined by inserting the value of n as follows:

$$\mu_1 = \frac{\varphi\Gamma\left(\frac{1-b_N}{b_N}\right)}{b_N a_N^{\frac{1-b_N}{b_N}}}\left[\frac{2}{(2u_N(n_N+1)+z_N+1)^{\frac{1-b_N}{b_N}}} - \frac{1}{(2u_N(n_N+1)+z_N+2)^{\frac{1-b_N}{b_N}}}\right] \quad (11)$$

$$\mu_2 = \frac{\varphi\Gamma\left(\frac{2-b_N}{b_N}\right)}{b_N a_N^{\frac{2-b_N}{b_N}}}\left[\frac{2}{(2u_N(n_N+1)+z_N+1)^{\frac{2-b_N}{b_N}}} - \frac{1}{(2u_N(n_N+1)+z_N+2)^{\frac{2-b_N}{b_N}}}\right] \quad (12)$$

$$\mu_3 = \frac{\varphi\Gamma\left(\frac{3-b_N}{b_N}\right)}{b_N a_N^{\frac{3-b_N}{b_N}}}\left[\frac{2}{(2u_N(n_N+1)+z_N+1)^{\frac{3-b_N}{b_N}}} - \frac{1}{(2u_N(n_N+1)+z_N+2)^{\frac{3-b_N}{b_N}}}\right] \quad (13)$$

$$\mu_4 = \frac{\varphi\Gamma\left(\frac{4-b_N}{b_N}\right)}{b_N a_N^{\frac{4-b_N}{b_N}}}\left[\frac{2}{(2u_N(n_N+1)+z_N+1)^{\frac{4-b_N}{b_N}}} - \frac{1}{(2u_N(n_N+1)+z_N+2)^{\frac{4-b_N}{b_N}}}\right] \quad (14)$$

From it, we can get the skewness and kurtosis of the NMWIW distribution as follows [22]:

$$SK = \frac{\frac{\varphi\Gamma\left(\frac{3-b_N}{b_N}\right)}{b_N a_N^{\frac{3-b_N}{b_N}}}\left[\frac{2}{(2u_N(n_N+1)+z_N+1)^{\frac{3-b_N}{b_N}}} - \frac{1}{(2u_N(n_N+1)+z_N+2)^{\frac{3-b_N}{b_N}}}\right]}{\left(\frac{\varphi\Gamma\left(\frac{2-b_N}{b_N}\right)}{b_N a_N^{\frac{2-b_N}{b_N}}}\left[\frac{2}{(2u_N(n_N+1)+z_N+1)^{\frac{2-b_N}{b_N}}} - \frac{1}{(2u_N(n_N+1)+z_N+2)^{\frac{2-b_N}{b_N}}}\right]\right)^{\frac{3}{2}}} \quad (15)$$

$$Ku = \frac{\frac{\varphi\Gamma\left(\frac{4-b_N}{b_N}\right)}{b_N a_N^{\frac{4-b_N}{b_N}}}\left[\frac{2}{(2u_N(n_N+1)+z_N+1)^{\frac{4-b_N}{b_N}}} - \frac{1}{(2u_N(n_N+1)+z_N+2)^{\frac{4-b_N}{b_N}}}\right]}{\left(\frac{\varphi\Gamma\left(\frac{2-b_N}{b_N}\right)}{b_N a_N^{\frac{2-b_N}{b_N}}}\left[\frac{2}{(2u_N(n_N+1)+z_N+1)^{\frac{2-b_N}{b_N}}} - \frac{1}{(2u_N(n_N+1)+z_N+2)^{\frac{2-b_N}{b_N}}}\right]\right)^{2}} - 3 \quad (16)$$

The table below presents the intervals for some moments of the NMWIW distribution. The table aims to display the variation in moments as the distribution parameter change, reflect the effect of varying the distribution parameter on the first four moment, and help analyze the properties of the neutrosophic distribution under uncertainty intervals, enabling an understanding of the statistical behavior of the distribution under fuzzy and uncertain data.

Table 2: Some intervals of neutrosophic moments for NMWIW distribution.

r_N	u_N	a_N	b_N	$\grave{\mu}_{1_N}$	$\grave{\mu}_{2_N}$	$\grave{\mu}_{3_N}$	$\grave{\mu}_{4_N}$	σ_N^2	S_N	K_N
[1.4,2.4]	[1.2,2.2]	[1.3, 2.3]	[1.1,2.1]	[1.985121, 1.815018]	[4.624668, 3.343843	[12.40814, 6.246785]	[37.70018, 11.82274]	[0.683963, 0.049553]	[1.24763, 1.021616]	[1.762716, 1.057369]
			[1.2,2.2]	[1.862946, 1.765914]	[3.975513, 3.1613]	[9.576761, 0.005713]	[25.69633, 10.51815]	[0.504945, 0.042848]	[1.208172, 0.001016]	[1.625866, 1.052466]
		[1.5, 2.5]	[1.3,2.3]	[1.972624, 1.785871]	[4.373004, 3.229522]	[10.7688, 5.909177]	[29.14297, 10.93223]	[0.481759, 0.040187]	[1.177599, 1.018168]	[1.523962, 1.048171]
			[1.4,2.4]	[1.871664, 1.742791]	[3.876852, 3.072545]	[8.804346, 5.47596]	[21.73056, 9.859563]	[0.373726, 0.035225]	[1.153396, 1.016747]	[1.445814, 1.044386]

	[1.5,2.5]	**[1.7, 2.7]**	**[1.5,2.5]**	[1.986465, 1.78014]	[4.194397, 3.196532]	[9.358978, 5.78711]	[21.95364, 10.55862]	[0.248354, 0.027634]	[1.089492, 1.012612]	[1.247865, 1.033354]
			[1.6,2.6]	[1.899532, 1.740805]	[3.80834, 3.054881]	[8.019649, 5.401849]	[17.66091, 9.620983]	[0.200118, 0.024479]	[1.079075, 1.011698]	[1.217704, 1.030934]
		[1.9,2.9]	**[1.7,2.7]**	[1.949842, 1.750911]	[3.989136, 3.088695]	[8.528279, 5.487342]	[18.982, 9.81449]	[0.187252, 0.023006]	[1.070393, 1.01088]	[1.192846, 1.028769]
			[1.8,2.8]	[1.876392, 1.716007]	[3.675888, 2.965262]	[7.492177, 5.157963]	[15.83754, 9.028642]	[0.155041, 0.020582]	[1.063077, 1.010145]	[1.172096, 1.026825]

The table shows that the moments vary significantly based on different values of their parameters. There is a discrepancy in the values between the upper and lower bounds of each moment, indicating the influence of the degree of neutrosophic uncertainty on the moment. The variation in skewness and kurtosis also shows how the shape of the distribution changes from a sharply skewed state to a flat distribution, reflecting the flexibility of the distribution in dealing with real data.

3. 3 Neutrosophic Moment Generating function for NMWIW distribution

Theorem: Let X_N be a neutrosophic random variable where $g(x_N)$ denotes the Npdf, then the neutrosophic Moment Generating Function of NMWIW distribution has the form:

$$M_x(t)=\sum_{r=0}^{\infty}\frac{t^r}{r!}\left[\Gamma\,\frac{\varphi\Gamma\left(\frac{n-b_N}{b_N}\right)}{b_N a_N^{\frac{n-b_N}{b_N}}}\left[\frac{2}{(2u_N(n_N+1)+z_N+1)^{\frac{n-b_N}{b_N}}}-\frac{1}{(2u_N(n_N+1)+z_N+2)^{\frac{n-b_N}{b_N}}}\right]\right] \tag{21}$$

Proof: Let X_N be a neutrosophic random variable, where $g(x_N)$ denotes the Npdf, then the neutrosophic Moment Generating Function given by form [23]:

$$M_x(t)=E(e^{tx})=\int_{-\infty}^{\infty}e^{tx}f(x_N)dx$$

Using exponential expansion for above equation, the we get a form:

$$M_x(t)=E(e^{tx})=\sum_{r=0}^{\infty}\frac{t^r}{r!}[\mu_n]$$

From Equation 14, the neutrosophic Moment Generating Function for the NMWIW distribution takes the form shown in Equation 21 ■.

3. 4 Neutrosophic Incomplete Moments function for NMWIW distribution

Theorem: Let X_N be a neutrosophic random variable, where $g(x_N)$ denotes the Npdf, then the neutrosophic Incomplete Moments function of NMWIW distribution has the form:

$$M_n(y)=\frac{2\varphi\Gamma\left(\left(\frac{n-b_N}{b_N}\right),(2u_N(n_N+1)+z_N+1)a_N y_N^{-b_N}\right)}{b_N a_N^{\frac{n-b_N}{b_N}}(2u_N(n_N+1)+z_N+1)^{\frac{n-b_N}{b_N}}}-\frac{\varphi\Gamma\left(\left(\frac{n-b_N}{b_N}\right),(2u_N(n_N+1)+z_N+2)a_N y_N^{-b_N}\right)}{b_N a_N^{\frac{n-b_N}{b_N}}(2u_N(n_N+1)+z_N+2)^{\frac{n-b_N}{b_N}}} \tag{22}$$

Proof: let X_N be an neutrosophic random variable with $g(x_N)$ is Npdf, then the neutrosophic Incomplete Moments function given by form [24]:

$$M_n(y)=\int_{-\infty}^{y}x^n f(x)dx$$

From equation 12, we get:

$$M_n(y)=\int_0^y x^n\left(2\varphi x_N^{-(b_N+1)}\left(e^{-a_N x_N^{-b_N}}\right)^{2u_N(n_N+1)+z_N+1}-\varphi x_N^{-(b_N+1)}\left(e^{-a_N x_N^{-b_N}}\right)^{2u_N(n_N+1)+z_N+2}\right)dx$$

$$M_n(y)=2\varphi I_1 dx_N-\varphi I_2 dx_N$$

where $I_1 = \int_0^y x_N^{n-(b_N+1)} \left(e^{-a_N x_N^{-b_N}}\right)^{2u_N(n_N+1)+z_N+1} dx_N$

and $I_2 = \int_0^y x_N^{n-(b_N+1)} \left(e^{-a_N x_N^{-b_N}}\right)^{2u_N(n_N+1)+z_N+2} dx_N$

For I_1, let $t = (2u_N(n_N+1)+z_N+1)a_N x_N^{-b_N}$

$x_N = \frac{t^{\frac{1}{b_N}}}{a_N^{\frac{1}{b_N}}(2u_N(n_N+1)+z_N+1)^{\frac{1}{b_N}}}$, when $x_N = 0 \Longrightarrow t = 0$ and if $x_N = y \Longrightarrow t = (2u_N(n_N+1)+z_N+1)a_N y_N^{-b_N} \Longrightarrow dy_N = \frac{\frac{1}{b_N} y^{\frac{1}{b_N}-1}}{a_N^{\frac{1}{b_N}}(2u_N(n_N+1)+z_N+1)^{\frac{1}{b_N}}} dt$

$$I_1 = \int_0^{(2u_N(n_N+1)+z_N+1)a_N y_N^{-b_N}} \left(\frac{t^{\frac{1}{b_N}}}{a_N^{\frac{1}{b_N}}(2u_N(n_N+1)+z_N+1)^{\frac{1}{b_N}}}\right)^{n-(b_N+1)} e^{-t} \frac{\frac{1}{b_N} y^{\frac{1}{b_N}-1}}{a_N^{\frac{1}{b_N}}(2u_N(n_N+1)+z_N+1)^{\frac{1}{b_N}}} dt$$

$$I_1 = \frac{\Gamma\left(\left(\frac{n-b_N}{b_N}\right), (2u_N(n_N+1)+z_N+1)a_N y_N^{-b_N}\right)}{b_N a_N^{\frac{n-b_N}{b_N}} (2u_N(n_N+1)+z_N+1)^{\frac{n-b_N}{b_N}}}$$

In the same way for I_2 to get a final form:

$$I_2 = \frac{\Gamma\left(\left(\frac{n-b_N}{b_N}\right), (2u_N(n_N+1)+z_N+2)a_N y_N^{-b_N}\right)}{b_N a_N^{\frac{n-b_N}{b_N}} (2u_N(n_N+1)+z_N+1)^{\frac{n-b_N}{b_N}}}$$

Then the neutrosophic Moment Generating Function for the NMWIW distribution has the form shown in Equation 22 ■.

3.1 Neutrosophic Characteristic function for NMWIW distribution

Theorem: Let X_N be a neutrosophic random variable, where $g(x_N)$ denotes the Npdf, then the neutrosophic Characteristic function of the NMWIW distribution has the form:

$$Q_{x_N}(t_N) = \sum_{v=0}^{\infty} \frac{(it_N)^v}{v!} \left[\frac{\varphi\Gamma\left(\frac{n-b_N}{b_N}\right)}{b_N a_N^{\frac{n-b_N}{b_N}}} \left[\frac{2}{(2u_N(n_N+1)+z_N+1)^{\frac{n-b_N}{b_N}}} - \frac{1}{(2u_N(n_N+1)+z_N+2)^{\frac{n-b_N}{b_N}}}\right]\right] \tag{23}$$

Proof: let X_N be a neutrosophic random variable with $g(x_N)$ is Npdf, then the neutrosophic Characteristic function given by form [25]:

$Q_{x_N}(t_N) = E(e^{it_N x_N}) = \int_0^{\infty} e^{it_N x_N} g(x_N)\, dx_N$

Using exponential expansion for above equation, the we get a form:

$Q_{x_N}(t_N) = E(e^{it_N x_N}) = \sum_{v=0}^{\infty} \frac{(it_N)^v}{v!} [\mu_n]$

From Equation 14, the neutrosophic Characteristic function for the NMWIW distribution takes the form shown in Equation 23 ■.

3. 5 Neutrosophic Rényi entropy for NMWIW distribution

Theorem Let X_N be a neutrosophic random variable, where $g(x_N)$ denotes the Npdf, then the neutrosophic Rényi entropy of the NMWIW distribution has the form:

$$I_R(c) = \frac{1}{1-c} log \left[Q\Gamma\left(\frac{1-c(b_N+1)}{b_N}\right)\right] \tag{17}$$

where $Q = \sum_{n=0}^{c} (-1)^n (c\ n) 2\varphi^{c-n}\varphi^n \frac{1}{b_N a^{\frac{-c(b_N+1)}{b_N}+\frac{1}{b_N}}((2u_N(n_N+1)+z_N+1)c+n)^{\frac{-c(b_N+1)}{b_N}+\frac{1}{b_N}}}$

Proof: let X_N be a neutrosophic random variable with $g(x_N)$ is Npdf, then the neutrosophic Rényi entropy given by form [26], [27]:

$$I_R(c) = \frac{1}{1-c} log \int_0^{\infty} g(x_N)^c dx$$

From equation 12, we get:

$$I_R(c) = \frac{1}{1-c} log \int_0^{\infty} \left(2\varphi x_N^{-(b_N+1)} \left(e^{-a_N x_N^{-b_N}}\right)^{2u_N(n_N+1)+z_N+1} - \varphi x_N^{-(b_N+1)} \left(e^{-a_N x_N^{-b_N}}\right)^{2u_N(n_N+1)+z_N+2}\right)^c dx_N$$

Using the Binomial Series

$$I_R(c)=\frac{1}{1-c}log\int_0^{\infty}\sum_{n=0}^{c}(-1)^n\,(c\;n\;)2\varphi^{c-n}\varphi^n x_N^{-c(b_N+1)}e^{-(2u_N(n_N+1)+z_N+1)c+n)\;a_N x_N^{-b_N}}\,dx_N$$

Let $u=(2u_N(n_N+1)+z_N+1)c+n)\;a_N x_N^{-b_N}\Longrightarrow x_N=\frac{u^{\frac{1}{b_N}}}{a^{\frac{1}{b_N}}((2u_N(n_N+1)+z_N+1)c+n)^{\frac{1}{b_N}}}$

$\Longrightarrow dx=\frac{\frac{1}{b_N}u^{\frac{1}{b_N}-1}}{a^{\frac{1}{b_N}}((2u_N(n_N+1)+z_N+1)c+n)^{\frac{1}{b_N}}}du$, to get:

$$I_R(c)=\frac{1}{1-c}log=\int_0^{\infty}\sum_{n=0}^{c}(-1)^n\,(c\;n\;)2\varphi^{c-n}\varphi^n\left(\frac{u^{\frac{1}{b_N}}}{a^{\frac{1}{b_N}}((2u_N(n_N+1)+z_N+1)c+n)^{\frac{1}{b_N}}}\right)^{-c(b_N+1)}\frac{\frac{1}{b_N}u^{\frac{1}{b_N}-1}e^{-u}}{a^{\frac{1}{b_N}}((2u_N(n_N+1)+z_N+1)c+n)^{\frac{1}{b_N}}}du$$

Put $Q=\sum_{n=0}^{c}(-1)^n\,(c\;n\;)2\varphi^{c-n}\varphi^n\frac{1}{b_N a^{\frac{-c(b_N+1)}{b_N}+\frac{1}{b_N}}((2u_N(n_N+1)+z_N+1)c+n)^{\frac{-c(b_N+1)}{b_N}+\frac{1}{b_N}}}$, then we get:

$$I_R(c)=\frac{1}{1-c}log\left[Q\int_0^{\infty}u^{\frac{-c(b_N+1)}{b_N}+\frac{1}{b_N}-1}\,e^{-u}du\right]$$

Then the neutrosophic Rényi entropy for the NMWIW distribution is given in Equation 24 ■.

4 Estimation

4. 1 Maximum Likelihood Estimation

Maximum likelihood estimate method is used to obtain the NMWIW distribution parameters. For the random sample $x_{N_1}, x_{N_2}, \dots, x_{N_m}$ [28, 29, 30]. The following is the NMWIW distribution Npdf:

$$L(\Theta,X_N)=\prod_{i=1}^{n}r_N u_N a_N b_N x_N^{-(b_N+1)}e^{-r_N\left(\frac{\left(e^{-a_N x_N^{-b_N}}\right)^2}{1-e^{-a_N x_N^{-b_N}}}\right)^{u_N}}\left(\frac{\left(e^{-a_N x_N^{-b_N}}\right)^2}{1-e^{-a_N x_N^{-b_N}}}\right)^{u_N-1}\left[\frac{2\left(e^{-a_N x_N^{-b_N}}\right)^2-\left(e^{-a_N x_N^{-b_N}}\right)^3}{\left(1-e^{-a_N x_N^{-b_N}}\right)^2}\right]$$

log-likelihood is calculated:

$$l=l(\Delta)=nlog(r_N)+nlog(u_N)+nlog(a_N)+nlog(b_N)-(b_N+1)\sum_{i=1}^{n}log\left(x_{N_i}\right)$$
$$-r_N\sum_{i=1}^{n}log\left[\left(\frac{\left(e^{-a_N x_N^{-b_N}}\right)^2}{1-e^{-a_N x_N^{-b_N}}}\right)^{u_N}\right]+(u_N-1)\sum_{i=1}^{n}log\left(\frac{\left(e^{-a_N x_N^{-b_N}}\right)^2}{1-e^{-a_N x_N^{-b_N}}}\right)+\sum_{i=1}^{n}log\left[\frac{2\left(e^{-a_N x_N^{-b_N}}\right)^2-\left(e^{-a_N x_N^{-b_N}}\right)^3}{\left(1-e^{-a_N x_N^{-b_N}}\right)^2}\right] \quad (18)$$

4. 2 Least Square Estimation

The Least squares estimation (LSE) method can be used to estimate a parameter using the following formula:

$$\varphi(\theta_N)=\sum_{i=1}^{m}\left[1-e^{-r_N\left(\frac{\left(e^{-a_N x_N^{-b_N}}\right)^2}{1-e^{-a_N x_N^{-b_N}}}\right)^{u_N}}-\frac{i}{n+1}\right]^2 \quad (26)$$

4. 3 Weight Least Squares Estimation

The Weight Least Squares Estimation (WLSE) technique can estimate a parameter using the following formula:

$$W(\theta_N)=\sum_{i=1}^{m}\frac{(n+1)^2(n+2)}{i(n-i+1)}\left[1-e^{-r_N\left(\frac{\left(e^{-a_N x_N^{-b_N}}\right)^2}{1-e^{-a_N x_N^{-b_N}}}\right)^{u_N}}-\frac{i}{n+1}\right]^2 \quad (27)$$

By computing that partial derivative with respect to the four parameters and setting them to zero, one can estimate the parameters using the three methods previously discussed in 25, 26, and 27. Due to the difficulty in identifying these values in numerical solution, computational tools such as the R programming language are employed.

5 Monte Carlo Simulation for NMWIW Distribution

Monte Carlo simulation is a mathematical method that uses random variables to model complicated systems and examine their behavior. This approach is extensively employed in disciplines like as statistics, economics, engineering, and the natural sciences. The fundamental premise of Monte Carlo simulation involves generating a substantial array of random samples to compute specified values or estimate probabilistic outcomes. This facilitates the examination of occurrences that are challenging to forecast by conventional mathematical techniques.

Monte Carlo simulation is important because of its ability to provide accurate estimates for complex models, especially when direct analytical solutions are difficult or impossible to obtain. Additionally, it may assess the performance or output of systems in uncertain situations or with imprecise data. The objective is to develop a Monte Carlo simulation technique for the NMWIW distribution, evaluating it across four sample sizes (50, 100, 150, and 200) and assessing its performance based on three criteria: MSE, RMSE, and bias [30]. The estimation will be conducted utilizing three methodologies: Maximum Likelihood Estimation (MLE), Least Squares Estimation (LSE), and Weighted Least Squares Estimation (WLSE). The folloing are fundamental stages for executing the simulation algorithm:

1. Random sample generation: Random samples were generated using the NMWIW distribution, with sample sizes of 50, 100, 150, and 200, while establishing beginning intervals for the parameters of the NMWIW distribution.

2. Estimation utilizing three methodologies: Maximum Likelihood Estimation (MLE), Least Squares Estimation (LSE), and Weighted Least Squares Estimation (WLSE), with WLSE incorporating varying weights for the data.

3. Assessment utilizing the subsequent criteria: Mean Squared Error (MSE): assesses the disparity between projected values and actual values. RMSE: The square root of the Mean Squared Error (MSE). Bias: The discrepancy between the projected value of the estimated value and the actual value.

4. The process is repeated several times to obtain reliable results.

5. Comparison of the three criteria: MSE, RMSE, and bias to determine the most accurate method

Table 3 presents the outcome values of Monte Carlo simulation for the NMWIW distribution.

Table 3: Outcome values of the Monte Carlo simulation for the NMWIW distribution.

$r_N = [2,3]$, $u_N = [2.3]$, $b_N = [5,6]$, $c_N = [3,4]$					
N	**Est.**	**Ess. Par.**	**MLE**	**LSE**	**WLSE**
50	Mean	$\widehat{r_N}$	[7.56595, 8.264537]	[2.4880443,3.5413582]	[2.5880582,3.7282819]
		$\widehat{u_N}$	[2.1089396,2.6072588]	[1.94482095,2.93480324]	[1.8989288,2.7927980]
		$\widehat{a_N}$	[8.131854,10.489774]	[5.5695093, 6.7064063]	[6.005062, 7.012677]
		$\widehat{b_N}$	[3.1268701,4.3925277]	[3.07385846,4.1202594]	[3.1394478,4.1691622]
	MSE	$\widehat{r_N}$	[130.82176,252.493083]	[3.4563565,4.1870320]	[3.5364616,9.8527928]
		$\widehat{u_N}$	[0.6801350,0.8630183]	[0.14200107,0.24075746]	[0.1913200,0.2675859]
		$\widehat{a_N}$	[50.525886,68.091033]	[3.5521445,3.9482269]	[5.481792,8.902501]
		$\widehat{b_N}$	[0.7005425,1.0133760]	[0.1747318,0.29914731	[0.3225176,0.5037847]
	RMSE	$\widehat{r_N}$	[11.43773,15.890031]	[1.8591279,2.0462238]	[1.8805482,3.1389159]
		$\widehat{u_N}$	[0.8247030,0.9289878]	[0.37683029,0.49067042]	[0.4374014,0.5172871]
		$\widehat{a_N}$	[7.108156,8.251729]	[1.8847134,1.9870146]	[2.341323,2.983706]
		$\widehat{b_N}$	[0.8369842,1.0066658]	[0.4180093,0.54694361]	[0.5679063,0.7097779]
	Bias	$\widehat{r_N}$	[4.56595,6.264537]	[0.4880443,0.5413582]	[0.5880582,0.7282819]
		$\widehat{u_N}$	[0.1089396,0.3927412]	[0.05517905,0.06519676]	[0.1010712,0.2072020]
		$\widehat{a_N}$	[3.131854,4.489774]	[0.5695093,0.7064063]	[1.005062,1.012677]
		$\widehat{b_N}$	[0.1268701,0.3925277]	[0.07385846,0.1202594]	[0.1394478,0.1691622]
100	Mean	$\widehat{r_N}$	[6.067012,6.563485]	[2.3625232,3.7830369]	[2.3943665,4.122681]
		$\widehat{u_N}$	[2.1186091,2.6639733]	[1.94104323,2.95404869]	[1.97696098,2.90000426]
		$\widehat{a_N}$	[7.175107,9.641682]	[5.5652552,6.2665734]	[5.6784151,6.3065592]
		$\widehat{b_N}$	[3.06519838,4.3303437]	[3.05657551,4.02116235]	[3.01591942,4.01692502]
	MSE	$\widehat{r_N}$	[71.701157,98.225053]	[0.7845137,5.2324155]	[1.8765938,8.904876]
		$\widehat{u_N}$	[0.5782823,0.6416282]	[0.08745089,0.11419794]	[0.16655280,0.18216329]
		$\widehat{a_N}$	[39.716860,44.163245]	[0.9021082,3.1420756]	[2.0786762,4.9023489]

		$\widehat{b_N}$	[0.6338395,0.77154591]	[0.05460942,0.22013825]	[0.06164051,0.18184659]
	RMSE	$\widehat{r_N}$	[8.467654, 9.910855]	[0.8857278, 2.2874474]	[1.3698882, 2.984104]
		$\widehat{u_N}$	[0.7604488, 0.8010170]	[0.29572096, 0.33793186]	[0.40810881, 0.42680592]
		$\widehat{a_N}$	[6.302131, 6.645543]	[0.9497938, 1.7725901]	[1.4417615, 2.2141249]
		$\widehat{b_N}$	[0.7961404, 0.87837686]	[0.23368659, 0.46918893]	[0.24827507, 0.42643474]
	Bias	$\widehat{r_N}$	[3.563485,4.067012]	[0.3625232, 0.7830369]	[0.3943665, 1.122681]
		$\widehat{u_N}$	[0.1186091, 0.3360267]	[0.04595131, 0.05895677]	[0.02303902, 0.09999574]
		$\widehat{a_N}$	[2.175107, 3.641682]	[0.2665734, 0.5652552]	[0.3065592, 0.6784151]
		$\widehat{b_N}$	[0.06519838, 0.3303437]	[0.02116235, 0.05657551]	[0.01591942, 0.01692502]
150	**Mean**	$\widehat{r_N}$	[5.656880, 5.851442]	[2.4527406, 3.5102294]	[2.8900622, 4.196943]
		$\widehat{u_N}$	[2.1316879, 2.7639804]	[1.98427918, 2.92490609]	[1.94769338, 2.8622271]
		$\widehat{a_N}$	[6.501664, 9.003176]	[5.1952284, 6.3508278]	[1.94769338, 6.7250552]
		$\widehat{b_N}$	[2.994000008,4.2057407]	[2.98828807, 4.02525019]	[3.05650448, 4.05515173]
	MSE	$\widehat{r_N}$	[48.838980, 58.552577]	[1.2160434, 3.1290169]	[3.3834773,11.021867]
		$\widehat{u_N}$	[0.5508149, 0.6011018]	[0.07758455, 0.11200368]	[0.1480497, 0.16610462]
		$\widehat{a_N}$	[24.685265, 36.015866]	[0.9324373, 1.5143428]	[3.0640409, 6.275008]
		$\widehat{b_N}$	[0.4481648,0.641311236]	[0.01953498, 0.08235943]	[0.04861499, 0.25563795]
	RMSE	$\widehat{r_N}$	[6.988489,7.651966]	[1.1027436, 1.7689027]	[1.8394231, 3.319920]
		$\widehat{u_N}$	[0.7421691,0.7753076]	[0.27854004, 0.33466950]	[0.3847723, 0.40755935]
		$\widehat{a_N}$	[4.968427,6.001322]	[0.9656280, 1.2305864]	[1.7504402, 2.504997]
		$\widehat{b_N}$	[0.6694511,0.800819103]	[0.13976761, 0.28698333]	[0.22048806, 0.50560652]
	Bias	$\widehat{r_N}$	[2.656880, 3.851442]	[0.4527406, 0.5102294]	[0.8900622, 1.196943]
		$\widehat{u_N}$	[0.1316879, 0.2360196]	[0.01572082, 0.07509391]	[0.05230662, 0.1377729]
		$\widehat{a_N}$	[1.501664, 3.003176]	[0.1952284, 0.3508278]	[0.7250552, 0.879842]
		$\widehat{b_N}$	[0.005999992,0.2057407]	[0.01171193, 0.02525019]	[0.05515173, 0.05650448]
200	**Mean**	$\widehat{r_N}$	[5.246874, 5.506475]	[2.2683086, 3.3525097]	[2.9763366, 3.9996271]
		$\widehat{u_N}$	[2.1733541, 2.7598669]	[2.005613975,2.92174345]	[2.0352894, 2.8346509]
		$\widehat{a_N}$	[6.054440, 8.771046]	[5.1790283, 6.2462197]	[5.3876513, 6.9018338]
		$\widehat{b_N}$	[2.94957927, 4.2061024]	[2.9993775194,4.02082663]	[2.97060468, 4.09181232]
	MSE	$\widehat{r_N}$	[35.528771, 53.060095]	[0.7351383, 2.4928414]	[3.8719163, 8.2974106]
		$\widehat{u_N}$	[0.5096972, 0.5863918]	[0.068979519, 0.07860993]	[0.1381748, 0.1680624]
		$\widehat{a_N}$	[18.042231, 31.712339]	[0.7045483, 1.4824716]	[2.8338271, 4.0403297]
		$\widehat{b_N}$	[0.4129333, 0.51841882]	[0.02340230,0.0807540095]	[0.04925460, 0.19230962]
	RMSE	$\widehat{r_N}$	[5.960602, 7.284236]	[0.8574020, 1.5788735]	[1.9677185, 2.8805226]
		$\widehat{u_N}$	[0.7139308,0.7657623]	[0.262639523, 0.28037463]	[0.3717187, 0.4099542]
		$\widehat{a_N}$	[4.247615,5.631371]	[0.8393737, 1.2175679]	[1.6833975, 2.0100571]
		$\widehat{b_N}$	[0.6425989, 0.72001307]	[0.15297810,0.2841724996]	[0.22193377, 0.43853121]
	Bias	$\widehat{r_N}$	[2.246874, 3.506475]	[0.2683086, 0.3525097]	[0.9763366, 0.9996271]
		$\widehat{u_N}$	[0.1733541, 0.2401331]	[0.005613975, 0.07825655]	[0.0352894, 0.1653491]
		$\widehat{a_N}$	[1.054440, 2.771046]	[0.1790283, 0.2462197]	[0.3876513, 0.9018338]
		$\widehat{b_N}$	[0.05042073, 0.2061024]	[0.0006224806,0.02082663]	[0.02939532, 0.09181232]

Table 3 presents the lost MSE and RMSE values for the MLE approach, indicating its superior accuracy. All approaches exhibit minimal bias, indicating the high quality of the estimation. Maximum Likelihood Estimation (MLE) demonstrated enhanced efficacy, particularly with an extensive sample size, establishing it as the optimal choice for the distribution. LSE and WLSE have strong performance with small sample size, although their accuracy diminishes as sample size grows.

6 Application by Real Data Set on NMWIW distribution

The practical aspect is crucial to illustrating the extent of the distribution's quality and effectiveness in real-world applications. In this section, a useful application is carried out on two types of actual neutrosophic the daily COVID-19 death rate in the Netherlands (March 31–April 30, 2020) [31], and estimated under-five mortality periods [32], and the results obtained are compared between the proposed distribution and six other distributions, which are represented by:

- neutrosophic beta with baseline inverse Weibull (NBIW),
- Neutrosophic Kumaraswamy with baseline inverse Weibull (NKIW),
- Neutrosophic Lomax with baseline inverse Weibull (NLIW),
- Neutrosophic generalized exponential with baseline inverse Weibull (NKIW),
- Neutrosophic Nadarajah-Haghighi with baseline inverse Weibull (NNIW),
- Neutrosophic inverse Weibull (NIW).

The reason for choosing these distributions is the similarity in mathematical structure and the ability to deal with uncertain data. All of the selected distribution belongs to families of extended or modified distribution of the Inverse Weibull distribution, which makes them direct competitors to the NMWIW. These distributions can represent ambiguous or uncertain data (which are expressed an intervals rather than specific values), which is the primary goal of the NMWIW.

AIC [20], CAIC [33, 34], HQIC [35, 36], and BIC [25] are four information criteria that were used in this comparison. Four accuracy statistical measures were also used, including: Kolmogorov-Smirnov (KS), Anderson-Darling (A), Cramér-von Mises (W), and p-value [15], [24].

Data set-I

Var	N	Mean	SD	Median	Trimmed	Mad	Min	Max	Range	SK	KU	Se
1	30	[6.14, 6.36]	[3.51, 3.56]	[5.37, 5.64]	[5.79, 6]	[2.72, 2.85]	[1.27, 1.34]	[14.92,15.66]	[13.64,14.33]	[0.8, 0.82]	[-0.18,0.3]	[0.64,0.65]

Tables 4-6 represent the results of comparing the seven distributions using accuracy and goodness-of-fit criteria, in addition to the results of estimating the parameters for each distribution using MLE.

Table 4: Results of the criteria for the distributions of dataset I.

Dist.	-2L	AIC	CAIC	BIC	HQIC
NMWIW	[75.55599,76.08404]	[159.112, 160.1681]	[160.712,161.7681]	[164.7168,165.7729]	[160.905, 161.9611]
NBIW	[78.29655,79.25393]	[164.5988,166.5154]	[166.1988,168.1154]	[170.2036,172.1202]	[166.3918,168.3084]
NKIW	[76.61699,77.25118]	[161.234,162.5024]	[162.834,164.1024]	[166.8388,168.1072]	[163.027,164.2954]
NEGIW	[78.80359,79.26546]	[165.6135,166.5362]	[167.2135,168.1362]	[171.2183,172.141]	[167.4065,168.3292]
NLIW	[76.51535,77.17052]	[161.0307,162.341]	[162.6307,163.941]	[166.6355,167.9458]	[162.8237,164.1341]
NNHIW	[83.9155,85.29191]	[175.8837,178.6214]	[177.4837,180.2214]	[181.4885,184.2262]	[177.6768,180.4145]
NIW	[80.908,81.86503]	[165.816,167.7301]	[166.2605,168.1745]	[168.6184,170.5325]	[166.7125,168.6266]

Table 4 demonstrates that NMWIW attained the lowest values across the majority of criteria, signifying its superior alignment with the data. The NNHIW distribution exhibited the lowest efficiency owing to its elevated values, while diminished criterion values augment the stability of the distribution when contrasting models of varying complexity.

Table 5: value of the statistical measures of dataset I.

Dist.	W	A	K-S	p-value
NMWIW	[0.03596197, 0.03723065]	[0.2231519, 0.2303865]	[0.09362781,0.1059051]	[0.854709, 0.9330473]
NBIW	[0.06382559,0.08087844]	[0.4690944, 0.5596681]	[0.111575, 0.1144379]	[0.7854589, 0.8097136]
NKIW	[0.02212384,0.02543978]	[0.1768067, 0.1914174]	[0.07170282,0.07541861]	[0.9906199, 0.9948427]
NEGIW	[0.07091353,0.07424767]	[0.5189132, 0.5216244]	[0.1078498, 0.1087248]	[0.832895, 0.8397911]
NLIW	[0.02135254,0.02300102]	[0.1611936, 0.1726823]	[0.07101487, 0.0722754]	[0.9943107, 0.9954307]
NNHIW	[0.1891266, 0.2052744]	[1.20147, 1.3047]	[0.09913166, 0.1089364]	[0.8312111, 0.9016092]
NIW	[0.1409066, 0.1590743]	[0.9393442, 1.032132]	[0.152061, 0.1532608]	[0.4379855, 0.4477796]

Table 5 indicates that NMWIW attained the greatest p-value and the lowest W and A values, demonstrating its superior fit to the data. Other distribution exhibited inferior performance relative to NMWIW

Table 6: Estimator value interval for parameters by MLE of dataset I.

Dist.	$\hat{r}_N$	$\hat{u}_N$	$\hat{a}_N$	$\hat{b}_N$
NMWIW	[0.05400885, 0.0547871]	[0.24783299, 0.2507718]	[11.35501098,20.8038998]	[7.26128426,7.4386287]
NBIW	[2.9764706, 3.0925537]	[4.2292581, 4.6259379]	[3.2801833, 3.2846942]	[0.7617259,0.7990768]
NKIW	[3.0336021, 3.1602180]	[54.1582469,82.3005852]	[3.0058539, 3.0864822]	[0.4127725,0.4404566]
NEGIW	[9.5149610, 10.1541193]	[1.9774360, 2.5250579]	[4.7101924, 5.5607849]	[0.5633951,0.5811702]
NLIW	[0.02443253, 0.0225292]	[17.25110260,17.8203001]	[5.61201003, 5.7854062]	[0.28521452,0.2864939]
NNHIW	[0.03653495, 0.2210295]	[-0.9912115, -0.99010004]	[22.96712404,23.0035338]	[3.2805157,3.30943424]
NIW	[7.847800, 8.576159]	[1.551447, 1.564117]	-------	--------

Table 6 presents the estimation intervals of the principal parameter of the NMWIW distribution in comparison to other distribution (such as NBIW, NKIW, etc.) utilizing the maximum likelihood estimation (MLE) approach for the initial dataset. The NMWIW distribution exhibited narrow parameter intervals, indicating the stability of its estimates, whereas other distributions, such as NBIW and NKIW, showed greater variability in parameter intervals, suggesting lower efficiency compared to NMWIW.

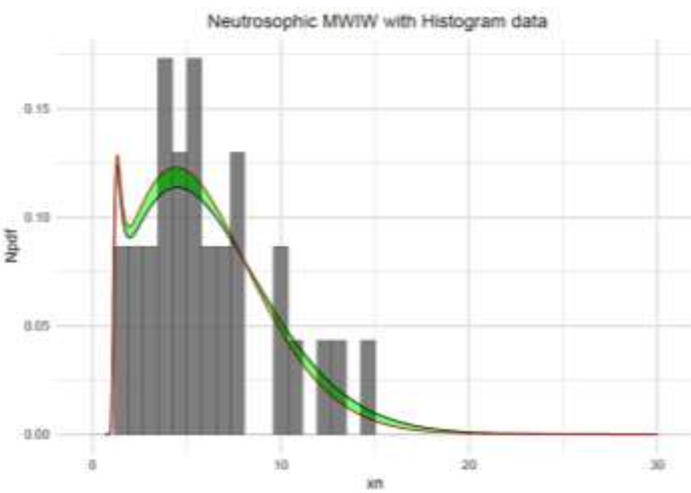

Figure 4: Fitting PDFs NMWIW with histogram data set.

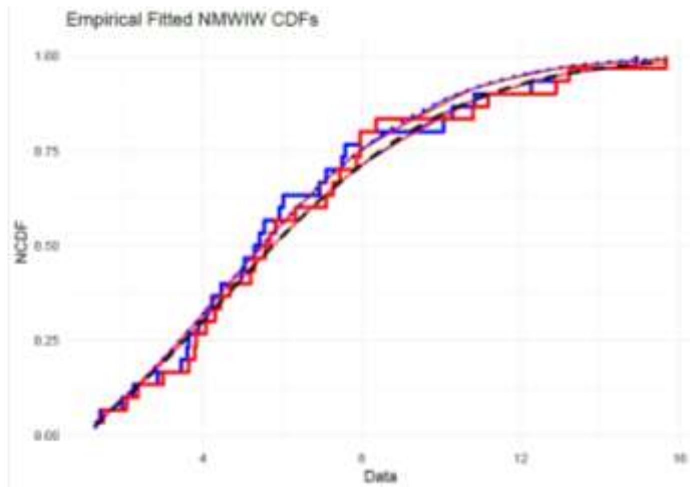

Figure 5: Empirical Fitted CDFs NMWIW with data set.

Figure 4 illustrates the alignment of the probability density function (PDF) of the NMWIW distribution with the empirical data for the initial dataset. The distribution exhibits a robust alignment with the overall structure of the data, as the curve conforms to the shape of the experimental data, demonstrating the capacity of NMWIW to correctly and adaptively represent actual data. Figure 5 illustrates the empirical cumulative distribution function (CDF) in comparison to the theoretical CDF. The robust alignment between the two distributions is apparent, demonstrating the capacity of NMWIW to depict the cumulative probability of data correctly.

Data set-II

Var	N	Mean	SD	Median	Trimmed	Mad	Min	Max	Range	SK	KU	Se
1	26	[15.76, 16.76]	[7.37, 7.27]	[14.21, 15.32]	[15.22, 16.26]	[8.27, 7.87]	[6.81, 7.98]	[31.53, 31.81]	[24.72, 23.83]	[0.56, 0.56]	[-0.93, -0.96]	[1.45, 1.43]

Tables 7-9 represent the results of comparing the seven distributions using accuracy and goodness-of-fit criteria, in addition to the results of estimating the parameters for each distribution using MLE.

Table 7: Results of the criteria for the distributions of dataset II.

Dist.	-L	AIC	CAIC	BIC	HQIC
NMWIW	[85.31004, 85.3712]	[178.6201,178.7424]	[180.5248, 180.6472]	[183.6525, 183.7748]	[180.0692, 180.1916]
NBIW	[85.82657, 85.6218]	[179.6531, 179.2436]	[181.5579, 181.1484]	[184.6855, 184.276]	[181.1023, 180.6927]
NKIW	[85.88461, 85.68361]	[179.7692, 179.3672]	[181.674, 181.272]	[184.8016, 184.3996]	[181.2184, 180.8164]
NEGIW	[85.96429, 85.77587]	[179.9286, 179.5517]	[181.8333, 181.4565]	[184.961, 184.5841]	[181.3777, 181.0009]
NLIW	[85.98495, 85.78574]	[179.9699, 179.5715]	[181.8747, 181.4762]	[185.0023, 184.6039]	[181.419, 181.0206]
NNHIW	[85.70042, 85.55605]	[179.4008, 179.1121]	[181.3056, 181.0169]	[181.666, 184.1445]	[180.85, 180.5612]
NIW	[87.97488, 89.04069]	[179.9497, 182.0814]	[182.4659, 182.6031]	[184.4659, 184.5976]	[180.67336, 182.806]

Table 7 shows that the NMWIW distribution demonstrated superior performance compared to other distributions (such as NBIW, NKIW, etc.), achieving the lowest values for information criteria such as AIC, CAIC, BIC, and HQIC. For example, the AIC values for NMWIW was in the range of 178.6201 to 178.7424, while it was much higher for other distribution such as NNHIW, which reached 179.4008 to 179.1121. These results suggest that NMWIW is more effective at representing real-world data under uncertain conditions, as lower parameter values reflect a better balance between model complexity and accuracy.

Table 8: Value of the statistical measures of dataset II.

Dist.	W	A	K-S	p-value
NMWIW	[0.03821282,0.0437546]	[0.3160439, 0.3897786]	[0.105938, 0.09644885]	[0.9027915, 0.9498353]
NBIW	[0.05307781, 0.04135859]	[0.3749891, 0.3352919]	[0.1005925, 0.1083155]	[0.9313852, 0.8884535]
NKIW	[0.05254187, 0.04118346]	[0.3739378, 0.3357333]	[0.8884535, 0.1063571]	[0.9064056, 0.9003333]
NEGIW	[0.05133014, 0.04308012]	[0.3718426, 0.3468346]	[0.109166, 0.105257]	[0.883098, 0.9067212]
NLIW	[0.05248551, 0.04137385]	[0.3762638, 0.3388238]	[0.1070826, 0.105434]	[0.8960071, 0.9057072]
NNHIW	[0.04809916, 0.03991631]	[0.350955, 0.3280546]	[0.1182845, 0.1034424]	[0.8190817, 0.9167904]
NIW	[0.06693629, 0.05156488]	[0.4487718, 0.3897633]	[0.1293297, 0.163349]	[0.7295865, 0.4447074]

Table 8 the NMWIW performed best on goodness of fit measures such as K-S and p-value, with the highest p-value (0.9027915, 0.9498353), indicating no evidence to reject the hypothesis that the model fits the data, It also had the lowest values for the Anderson-Darling (A) and Cremer–von Mises (W) metrics, confirming its ability to mimic the actual data distribution accurately. In comparison, the NIW distribution showed poor performance with p-values (0.7295865, 0.4447074), indicating its unsuitable for this dataset.

Table 9: Estimator value interval for parameters by MLE of dataset II.

Dist.	$\hat{r}_N$	$\hat{u}_N$	$\hat{a}_N$	$\hat{b}_N$
NMWIW	[0.3763069, 0.6708336]	[0.9691285, 1.0733202]	[25.8016873, 22.3779478]	[1.6367890, 1.4049113]
NBIW	[13.2524126, 13.875188]	[16.3963211, 14.152517]	[3.4613962, 4.059859]	[0.5523993, 0.646267]
NKIW	[6.5300683, 9.702639]	[8.3708336, 7.020073]	[4.7151010, 4.759534]	[0.9445675, 1.093304]
NEGIW	[36.8596699, 39.9847668]	[0.7559911, 5.4482379]	[27.0159664, 8.8413262]	[0.6904264, 0.4069596]
NLIW	[2.0224036, 2.9191380]	[25.0074481, 27.8838125]	[12.0188809, 17.2014241]	[0.7846065, 0.9245617]
NNHIW	[10.2879695, 11.6154147]	[0.4302104, 0.3563667]	[25.6349516, 35.6783356]	[0.9312000, 1.0386221]
NIW	------	-----	[99.403537, 88.963650]	[1.905606, 1.795603]

Table 9, the NMWIW parameters showed remarkable stability, with their estimation intervals being narrower compared to other distributions. For example, the shape parameter b_N was in the range 1.6367890 to 1.4049113, while it was much broader in the NKIW distribution (0.4127725 to 0.4404566). This suggests greater stability in the NMWIW estimates, enhancing its reliability in statistical modeling.

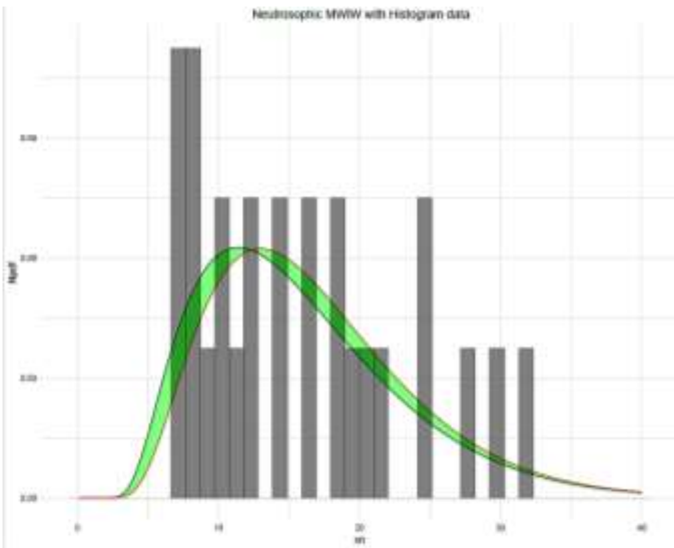

Figure 6: Fitting PDFs NMWIW with histogram dataset II.

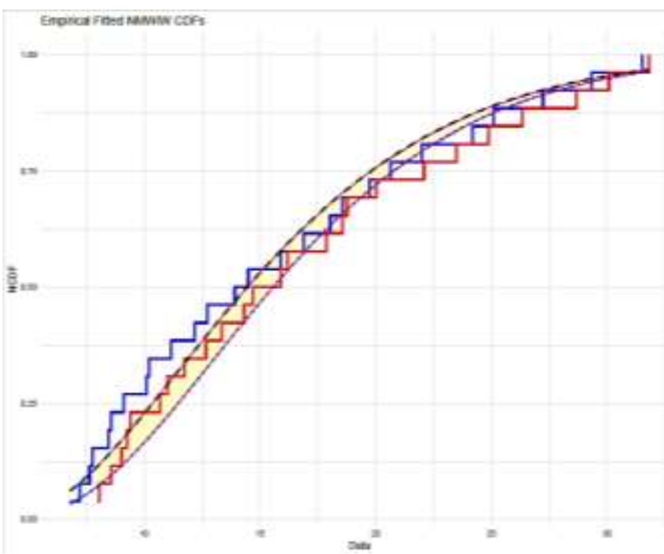

Figure 7: Empirical Fitted CDFs NMWIW with data set-II.

Figure 6 shows an explicit agreement between the NPDF of the NMWIW and the empirical histogram of the data, confirming the model's ability to capture the proper distribution of the data, especially in the tails of the distribution where the NMWIW demonstrates high flexibility in representing outliers. Figure 7 shows a near-perfect agreement between the theoretical NMWIW NCDF and the empirical distribution, supporting the hypothesis that the model is able to accurately represent the cumulative behavior of the data, even under uncertain conditions.

Conclusion

The NMWIW distribution outperformed competing distributions in representing uncertain data, as demonstrated by its low AIC and BIC values and high goodness of fit metrics (e.g., high p-value). The ability to represent diverse data behavior (e.g., heavy tails and asymmetric distributions) is enhanced by uncertainty parameters that provide ranges rather than fixed values. The model successfully analyzed sensitive data such as COVID-19 death and infant mortality, making it suitable for medical and social applications where data are uncertain. Parameter estimates using MLE were the most stable, especially with increasing sample size, as demonstrated by Monte-Carlo simulations. The distribution can be extended to include multidimensional data or combined with machine learning techniques to improve predictions under uncertainty. The NMWIW model was developed within the framework of neutrosophic logic rather than relying on classical distributions. This is because classical distributions (such as the traditional inverse Weibull) assume that the data are precise and defined by fixed values, which is an unrealistic assumption in many practical applications (such as epidemic data or medical estimates). The neutrosophic distribution also allows data to be represented as intervals, which better reflects the ambiguity and variability of real-world measurements. These results provide a qualitative addition to the field of statistical modeling of ambiguous data and open new avenues for applications in public health and the social sciences.

References

[1] Afifya, A. Z., Corderio, G. M., Yousof, H. M., Nofal, Z. M. and Alzaatreh, A. The Kumaraswamy transmuted-G family of distributions: properties and applications. *Journal of Data Science* **14**(2), 245-270, 2016.

[2] Afify, A. Z., Altum, E., Alizadeh, M., Ozel, G. and Hamedani, G. G. The odd exponentiated half-logistic-G family: properties, characterizations and applications. *Chilean Journal of Statistics* **8**(2), 65-91, 2017.

[3] Nasiru, S. Extended odd Frechet-G family of distributions. *Journal of Probability and Statistics* **11**(4), 1–12, 2018.

[4] DJIBRILA, S. The generalized odd inverted exponential-G family of distributions: properties and applications. *Eurasian Bulletin of Mathematics*, 86-110, 2019.

[5] Walid, E. and Tashkandy, Y. Modeling the amount of carbon dioxide emissions application: New modified alpha power Weibull-X family of distributions. *Symmetry* **15**(2), 366, 2023.

[6] Noori, N. A., Khalaf, A. A. and Khaleel, M. A. A New Generalized Family of Odd Lomax-G Distributions Properties and Applications. *Advances in the Theory of Nonlinear Analysis and Its Application* **7**(4), 1-16, 2023.

[7] Odeyale, A. B., Gulumbe, S. U., Umar, U, and Aremu, K. O. New New Odd Generalized Exponentiated Exponential-G Family of Distributions. *UMYU Scientifica* **2**(4), 56-64, 2023.

[8] Shah, Z., Khan D. M., Khan, Z., Faiz, N., Hussain, S., Anwar, A., Ahmad, T. and Kim, K.-I. A new generalized logarithmic–X family of distributions with biomedical data analysis. *Applied Sciences* **13**(6), 3668, 2023.

[9] Bello, O. A., Doguwa, S. I., Yahaya A. and Jibril, H. M. A type I half Logistic exponentiated-G family of distributions: Properties and application. *Communication in Physical Sciences* **7**(3), 147-163, 2021.

[10] Mahdi, G. A., Khaleel, M. A., Gemeay, A. M., Nagy, M., Mansi, A. H., Hossain, M. M., and Hussam, E. A new hybrid odd

exponential-Φ family: Properties and applications. *AIP Advances* **14(**4), 2024.

[11] Smarandache, F. A unifying field in logics. Neutrosophy: Neutrosophic probability, set and logic. *Rehoboth*, 1999.

[12] Alanaz, M. M., Mustafa, M. Y. and Algamal,Z. Y. Neutrosophic Lindley distribution with application for Alloying Metal Melting Point. *International Journal of Neutrosophic Science* **21**(4), 65-71, 2023.

[13] Algama, Z. Y., Alobaidi, N. N., Hamad, A. A., Alanaz, M. M. and Mustafa,M. Y. Neutrosophic Beta-Lindley distribution: Mathematical properties and modeling bladder cancer data. *International Journal of Neutrosophic Science* **23**(2), 186-194, 2024.

[14] Alanaz, M. M. and Algamal,Z. Y. Neutrosophic exponentiated inverse Rayleigh distribution: Properties and Applications. *International Journal of Neutrosophic Science* **21**(4), 36-43, 2023.

[15] Al-Saqal, O. E., Hadied, Z. A. and Algamal,Z. Y. Modeling bladder cancer survival function based on neutrosophic inverse Gompertz distribution. *International Journal of Neutrosophic Science* **25**(1), 75-5, 2025.

[16] Hammood, N. M., Rashad, N. K. and Algamal, Z. Y. Neutrosophic Topp-Leone Extended Exponential distribution modeling with application for bladder cancer patients. *International Journal of Neutrosophic Science* **25**(1), 239-245, 2025.

[17] Mustafa, M. Y. and Algamal, Z. Y. Neutrosophic inverse power Lindley distribution: A modeling and application for bladder cancer patients. *International Journal of Neutrosophic Science* **21**(2), 216-223, 2023.

[18] Noori, N. A., Khalaf, A. A. and Khaleel, M. A. A new expansion of the Inverse Weibull Distribution: Properties with Applications. *Iraqi Statistians Journal* **1**(1), 52-62, 1 1 2024.

[19] Noori,N. A. Exploring the Properties, Simulation, and Applications of the Odd Burr XII Gompertz Distribution. *Advances in the Theory of Nonlinear Analysis and Its Application* **7**(4), 60-75, 2023.

[20] Khaleel, M. A., Oguntunde, P. E., Al Abbasi, J. N., Ibrahim, N. A. and AbuJarad, M. H. The Marshall-Olkin Topp Leone-G family of distributions: A family for generalizing probability models. *Scientific African* **8**, e00470, 2020.

[21] Solomon Sarpong, A. L. and Nasiru, S. Odd Chen-G family of distributions. *Annals of Data Science* **9**(2), 369-391, 2022.

[22] Khalaf, A. A., Ibrahim, M. Q. and Noori, N. A. [0,1]Truncated Exponentiated Exponential Burr type X Distributionwith Applications. *Iraqi Journal of Science* **65**(8), 4428-4440, 2024.

[23] Gómez, H. J., Santoro, K. I., Chamorro, I. B., Venegas, O., Gallardo, D. I. and Gómez,H. W. A Family of Truncated Positive Distributions. *Mathematics* **11**(21), 4431, 2023.

[24] Noori, N. A., Khalaf, A. A. and Khaleel, M. A. A new expansion of the Inverse Weibull Distribution: Properties with Applications. *Iraqi Statistians Journal* **1**(1), 52-62, 2024.

[25] Aboraya, M. A new one-parameter G family of compound distributions: copulas, statistical properties and applications. *Statistics, Optimization & Information Computing, forthcoming* **9**, 942–962, 2021.

[26] Al-Habib, K. H., Khaleel, M. A. and Al-Mofleh, H. A new family of truncated nadarajah-haghighi-g properties with real data applications. *Tikrit Journal of Administrative and Economic Sciences* **19**(61), 2, 2023.

[27] Handique, L., ul Haq, M. A. and Subrata,C. Generalized Modified exponential-G family of distributions: its properties and applications. *International Journal of Mathematics and Statistics* **21**(1), 1-17, 2020.

[28] Afify, A. Z. , Yousof, H. and Nadarajah,S. The beta transmuted-H family for lifetime data. *Statistics and its Interface* **10**(3), 505-520, 2017.

[29] Chipepa, F., Oluyede, B. O. and Makubate, B. A New Generalized Family of Odd Lindley-G Distributions With Application. *International Journal of Statistics and Probability* **8**(6), 1-23, 2019.

[30] Bhatti, F. A., Hamedani, G. G., Korkmaz, M. C., Cordeiro, G. M., Yousof, H. M. and Ahmad, M. On Burr III Marshal Olkin family: development, properties, characterizations and applications. *Journal of Statistical Distributions and Applications* **6**, 1-21, 2019.

[31] Almongy, H. M., Almetwally, E. M., Aljohani, H. M., Alghamdi, A. S. and Hafez, E. H. A new extended Rayleigh distribution with applications of COVID-19 data. *Results in Physics* **23**, 104012, 2021.

[32] Zahid, K. , Almazah, M. M. A. , Odhah, O. H. and Alshanbari,H. M. Generalized pareto model: properties and applications in neutrosophic data modeling. Mathematical Problems in Engineering. *Mathematical Problems in Engineering* **1**, 3686968, 2022.

[33] Rahman, M. M., Gemeay, A. M., Khan, M. A. I., Meraou, M. A., Bakr, M. E., Muse, Hussam, A. H., E. and Balogun,O. S. A new modified cubic transmuted-G family of distributions: Properties and different methods of estimation with applications to real-life data. *AIP Advances* **13**(9), 095025, 2023.

[34] Oguntunde, P. E., Khaleel, M. A., Okagbue, H. I. and Odetunmibi,O. A. The Topp–Leone Lomax (TLLo) distribution with applications to airbone communication transceiver dataset. *Wireless Personal Communications*, 349-360, 2019.

[35] Cordeiro, G. M., Alizadeh, M., Ramires, T. G. and Ortega,E. M. M. The generalized odd half-Cauchy family of distributions: Properties and applications. *Communications in Statistics-Theory and Methods* **46**(11), 5685-5705, 2017.

[36] Abid, S. and Abdulrazak,R. [0, 1] truncated Frechet-Weibull and Frechet distributions. *International Journal of Research in Industrial Engineering* **7**(1), 106-135, 2018.

[37] Naz, S., Al-Essa, L. A., Bakouch, H. S. and Chesneau,C. A transmuted modified power-generated family of distributions with practice on submodels in insurance and reliability. *Symmetry* **15**(7), 1458, 7 15 2023.

[38] Khan, Z., M. Almazah, M. A., Odhah, O. H. and Alshanbari,H. M. Generalized Pareto Model: Properties and Applications in Neutrosophic Data Modeling. *Mathematical Problems in Engineering* **1**, 3686968, 2022.

[39] Hussain, S., Hassan, M. U., Rashid, M. S. and Ahmed,R. Families of Extended Exponentiated Generalized Distributions and Applications of Medical Data Using Burr III Extended Exponentiated Weibull Distribution. *Mathematics* **11**(14), 3090, 2023.

[40] Hussain, S., Hassan, M. U., Rashid, M. S. and Ahmed,R. Families of Extended Exponentiated Generalized Distributions and Applications of Medical Data Using Burr III Extended Exponentiated Weibull Distribution. *Mathematics* **11**(14), 3090, 2023.

[41] Sadiq, I. A., Doguwa, S. I., Yahaya, A. and Garba, J. New Generalized Odd Fréchet-G (NGOF-G) Family of Distribution with Statistical Properties and Applications. *UMYU Scientifica* **2**(3), 100-107, 2023.

[42] Abdelall, Y. Y., Hassan, A. S. and Almetwally, E. M. A new extention of the odd inverse Weibull-G family of distributions: Bayesian and non-Bayesian estimation with engineering applications. *Computational Journal of Mathematical and Statistical Sciences* **3**(2), 359-388, 2 3 2024.

[43] Ishaq, A. I., Panitanarak, U., Alfred, A. A. , Suleiman, A. A. and Daud, H. The Generalized Odd Maxwell-Kumaraswamy Distribution: Its Properties and Applications. *Contemporary Mathematics*, 711-742, 2024.

[44] Noori, N. A. and khaleel, M. A. Estimation and Some Statistical Properties of the hybrid Weibull Inverse Burr Type X Distribution with Application to Cancer Patient Data. *Iraqi Statisticians Journal* **1**(2), 8-29, 2024.

[45] Alzaatreh, Lee, A. C. and Famoye, F. A new method for generating families of continuous distributions. *Metron* **71**, 63–79, 2013.